

## Upper Crustal Velocity and Density Models Along FIRE4 Profile, Northern Finland

Hanna Silvennoinen<sup>1,2</sup>, Elena Kozlovskaya<sup>1</sup>, Jukka Yliniemi<sup>1</sup> and Timo Tiira<sup>3</sup>

<sup>1</sup> Sodankylä Geophysical Observatory/Oulu Unit, POB 3000, FIN-90014, University of Oulu, Finland

<sup>2</sup> Department of Physics, Division of Geophysics, POB 3000, FIN-90014, University of Oulu, Finland

<sup>3</sup> Institute of Seismology, POB 68, FIN-00014, University of Helsinki, Finland

(Received: September 2008; Accepted: May 2009)

### *Abstract*

*This study presents results of interpretation of wide-angle measurement of Vibroseis signals along the southern part of FIRE4 profile located in the northern Finland. The study was complemented by 3D density modelling of the area around the profile. The Finnish Reflection Experiment (FIRE) was a deep CMP reflection seismic survey made by Vibroseis technique along four transects in Finland during 2001–2003. During the experiment thirteen portable recording stations were deployed along FIRE4 profile in order to record wide-angle reflected and refracted waves generated by vibrator sources. These recordings were used to identify major refracted and reflected P-waves and to obtain a P-wave velocity model of the uppermost crust with both forward raytrace modelling and inversion. A model shows that the major geological units crossed by the profile can be distinguished as horizontal variations in the P-wave velocity values. The most interesting feature in a velocity model is a zone of high P-wave velocity below the Central Lapland Granitoid Complex at a depth of about 2 km. The area is marked by high reflectivity and correlates well with a large-scale maximum of the Bouguer anomaly. In order to constrain the depth of this feature and explain it in terms of rock composition, we applied modelling and inversion of Bouguer anomaly and calculated a 3D density model of the uppermost crust for the area around the profile. The modelling showed that the source of this anomaly is a high density body in the uppermost crust. Together with high reflectivity these density and velocity values could indicate that the Central Lapland Granitoid Complex is underlain by a highly deformed and folded structure composed of rocks with contrasting elastic properties.*

*Key words: Fennoscandia, wide-angle refraction and reflection seismics, Vibroseis, Bouguer anomaly, P-wave velocity modelling, P-wave velocity inversion, 3D density modelling*

### *1. Introduction*

Since 1980, seismic reflection experiments using Vibroseis sources have been widely used in lithospheric studies (Brown *et al.*, 1986, Blundel, 1990, DEKORP-Research Group, 1985, Bois *et al.*, 1988). In addition to information on reflectors in the crust and upper mantle, such experiments produce redundant amount of information on velocity that can be extracted from arrivals of refracted P-waves. However, this information is not very often utilized. Typically, 2D first arrival tomography is used to estimate velocities for pre-stack migration of the high-resolution reflection data (Rühl and Lüschen, 1990), while the usage of Vibroseis sources in wide-angle seismic reflection and refraction studies is limited to few cases (DEKORP RESEARCH GROUP,

1990, *Fomin and Goleby, 2007, Kukkonen et al., 2006*). However, the arrivals of refracted and wide-angle reflected waves can be used to model detailed velocity structure of the upper crust. In combination with near vertical reflection data, this enables a more detailed geological interpretation.

In our study, we present results of interpretation of wide-angle measurement of Vibroseis signals along FIRE4 profile (Fig. 1). The Finnish Reflection Experiment (FIRE) was a Vibroseis reflection seismic experiment, in which data were acquired in 2001–2003 along four transects. FIRE4 transect is situated in northern Finland, while other three profiles are in southern and central Finland. The transect consists of two long profiles (FIRE4 and FIRE4A) and short FIRE4B profile (Fig. 1).

Compared to the southern part, the northern part of Finland is poorly covered by seismic experiments. The previous seismic works included wide-angle reflection and refraction profiles POLAR (*Luosto et al., 1984, Walther and Flüh, 1993, Janik et al., 2009*), FINLAP (*Luosto et al., 1980*) and HUKKA (*Janik et al., 2009*). However, the southern part of FIRE 4 transect (FIRE4 profile) is situated in an area of very scarce seismic or other geophysical studies on a crustal scale. The only previous seismic profile there was HUKKA wide-angle reflection and refraction profile, with one shot point only. The seismic data along this profile was collected during three deployments in 1990–1995, but only recently a 1-D velocity model of this profile was published (*Janik et al., 2009*).

During FIRE experiment, the wide-angle reflection and refraction waves from Vibroseis sources were recorded along FIRE3 and FIRE4 profiles. The measurements were carried out by the Sodankylä Geophysical Observatory of the University of Oulu and Institute of Seismology of the University of Helsinki. The seismic contractor of the project was Spetsgeofizika S.E. (*Kukkonen et al., 2006*). The first purpose of the experiment was to test the possibility to record wide-angle reflection and refraction seismic signal from Vibroseis source with 1 Hz and 2 Hz geophones. The second task was to use these arrivals for the purpose of velocity modelling.

In our study, we analysed the wide-angle data recorded along FIRE4 profile and obtained a 2D velocity model of the uppermost crust. We used also 3D gravity modelling in order to obtain a 3D density model of the uppermost crust for the area around FIRE4 profile and to understand better the nature of the velocity variations obtained.

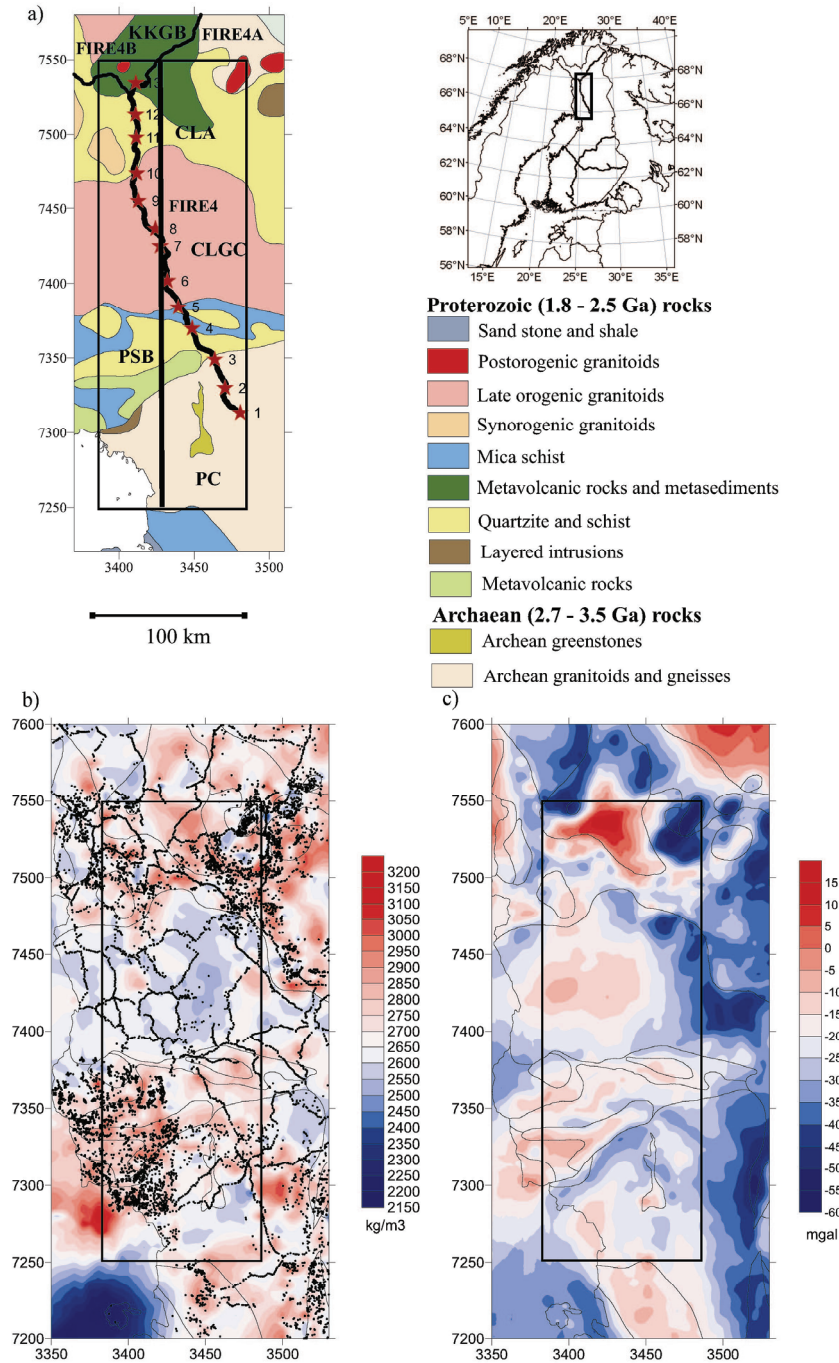


Fig. 1. The research area. (a) Position of FIRE4 and its extensions FIRE4B and part of FIRE4A on a geological map of Fennoscandian Shield (after *Koistinen et al.*, 2001 and *GTK*, 2003). The receiver points are marked with black stars on the map and the research area is marked with black rectangle and gravity profile with black line. The main geological units are PC – Pudasjärvi Complex, PSB – Peräpohja Schist Belt, CLGC – Central Lapland Granitoid Complex, CLA – Central Lapland Area, KKGB – Karasjok-Kittilä Greenstone Belt. The inset map of the Fennoscandia shows all FIRE profiles and the location of the research area. (b) The density map of the research area with black lines indicating the borders of geological units. The sample locations are shown with black dots. (c) The Bouguer anomaly map of research area (after *Korhonen et al.*, 2002). The average linear spacing of the gravity observations stations was 5 km and the Bouguer anomaly map used in this study is defined on 10 x 10 km<sup>2</sup> regular grid. The borders of main geological units are taken from *Koistinen et al.* (2001).

## 2. *Geological setting*

The study area (Fig. 1) is located in Fennoscandian Shield, northern Finland, with both Archean and Paleoproterozoic units. The Archean Karelian Craton forms the core of the Fennoscandian Shield and it is flanked from the north by Lapland-Kola Orogeny (Lahtinen *et al.*, 2008, Daly *et al.*, 2006). From south to north the research area crosses the Archean Pudasjärvi Complex belonging to Karelian Craton, and Paleoproterozoic Peräpohja Schist Belt, Central Lapland Granitoid Complex and Central Lapland Area (Patisson *et al.*, 2006).

The Pudasjärvi Complex is the only part of the research area where the Archean is not covered with younger units. It is one of the oldest crustal blocks Finland with ages ranging from 3.5 Ga (oldest rock ages in Finland) to 2.7 Ga (Huhma *et al.*, 2004). It is mainly composed of granitoids, migmatites and grey gneisses with some amphibolitic intrusions. Paleoproterozoic diabase and granitic dykes of different age groups intersect Pudasjärvi Complex (Koistinen *et al.*, 2001, Lehtinen *et al.*, 2005, Gaál and Gorbatshev, 1987).

The Peräpohja Schist Belt was formed about 2.5–1.9 Ga ago. It is a volcano-sedimentary basin with rocks belonging two age groups. The older group in the south was formed 2.5–2.1 Ga ago. It consists of terrestrial metasediments and metatholeiites. The younger group is 2.0–1.9 Ga old and it consists mainly of metasediments (Patisson *et al.*, 2006, Koistinen *et al.*, 2001, Lehtinen *et al.*, 2005, Gaál and Gorbatshev, 1987).

The Central Lapland Granitoid Complex has been formed in the Palaeoproterozoic around 1.8 Ga. The area is not well exposed, but granites and pegmatites are major rock types on outcrops (Patisson *et al.*, 2006, Koistinen *et al.*, 2001, Lehtinen *et al.*, 2005).

The Central Lapland Area is composed of Palaeoproterozoic metasediments intruded by granitoids (2.2–1.8 Ga ago). A part of Central Lapland Area is Karasjok-Kittilä Greenstone Belt. The Greenstone Belt marks the northern end of the research area. Karasjok-Kittilä Greenstone Belt is characterized by mafic and ultramafic volcanic rocks that were formed about 2.1 Ga ago (Gaál *et al.*, 1989).

Mineral prospecting, especially gold prospecting is active in the area and multiple gold prospects have been found in Peräpohja Shist Belt and Central Lapland Area, the most prominent ones in the Karasjok-Kittilä Greenstone Belt area (Eilu *et al.*, 2003).

## 3. *FIRE4 wide-angle reflection and refraction data acquisition and processing*

In FIRE experiment, the seismic signals were generated by five Vibroseis trucks each weighing 15.4 tons with maximum force limited to 60 % of the Vibroseis weight (Kukkonen *et al.*, 2006). The applied signal was a linear sweep ranging from 12 to 80 Hz. The duration of the sweep was 30 s. The vibration was repeated eight times at each point and the distance between vibration points along line was 100 m. The acquired near-vertical incidence data quality was good.

In addition, the wide-angle reflection and refraction survey was made along profiles FIRE3 and FIRE4 using the vibrators as a source. FIRE4 wide-angle reflection and refraction profile is 235 km long (Fig. 1). The seismic signal was recorded by thirteen portable seismic stations (Table 1). The experiment was carried out in winter conditions, which made it difficult to find high quality sites for seismic stations. Therefore only two from thirteen sites were on the bedrock. The sampling rate of portable stations (Reftek 72A) was 100 samples/s. The seismometers were Lennartz LE-3D (1 Hz) and Mark L-4A (2 Hz).

Table 1. The coordinates of the recording stations along FIRE4 wide-angle reflection and refraction profile. The coordinate system is the National Finnish Coordinate System (KKJ) (*Hirvonen, 1949; Ollikainen et al., 2001*). Also distances of the stations both from the beginning of FIRE4 reflection profile and from the previous station are shown as well as average, maximum and minimum distance between stations.

Recording stations	Coordinates (km)		Distances (km)	
	X	Y	On profile	Between stations
1	3480.714	7313.322	-4.421	
2	3470.539	7329.876	15.010	19.431
3	3463.700	7348.904	35.229	20.220
4	3448.631	7369.685	60.899	25.670
5	3439.352	7383.958	77.923	17.024
6	3432.161	7401.724	97.089	19.166
7	3427.287	7424.939	120.811	23.721
8	3424.159	7436.428	132.718	11.907
9	3412.718	7455.062	154.584	21.866
10	3411.736	7473.981	173.529	18.945
11	3411.329	7497.814	197.365	23.836
12	3410.930	7513.128	212.685	15.320
13	3411.100	7534.068	233.625	20.940
			Average	19.837
			Maximum	25.670
			Minimum	11.907

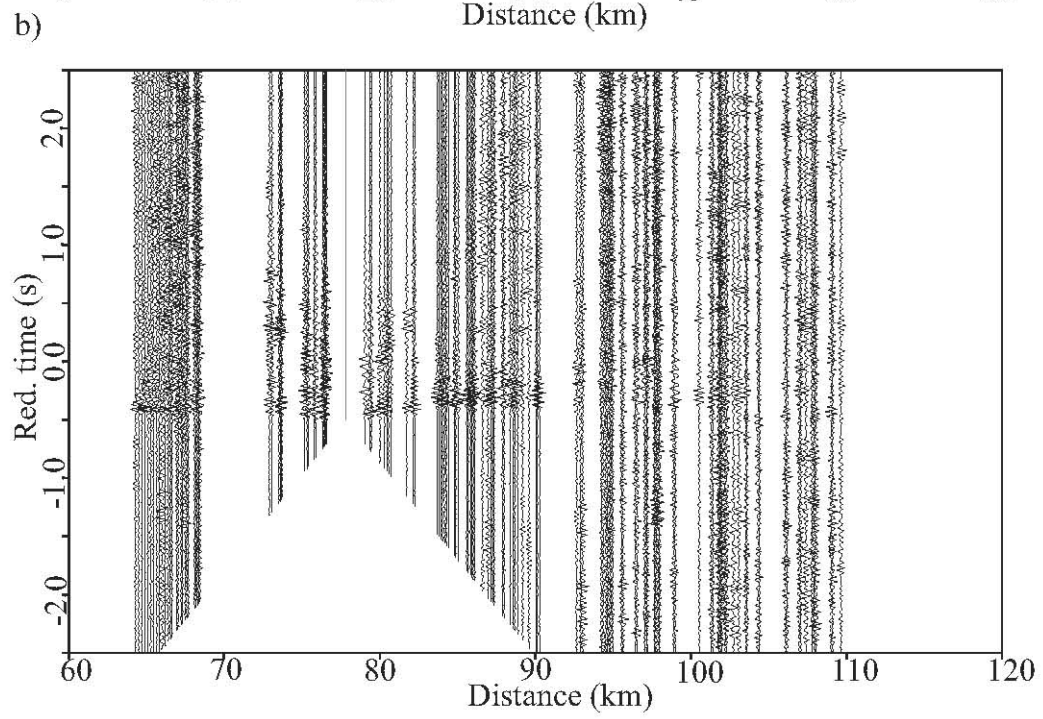
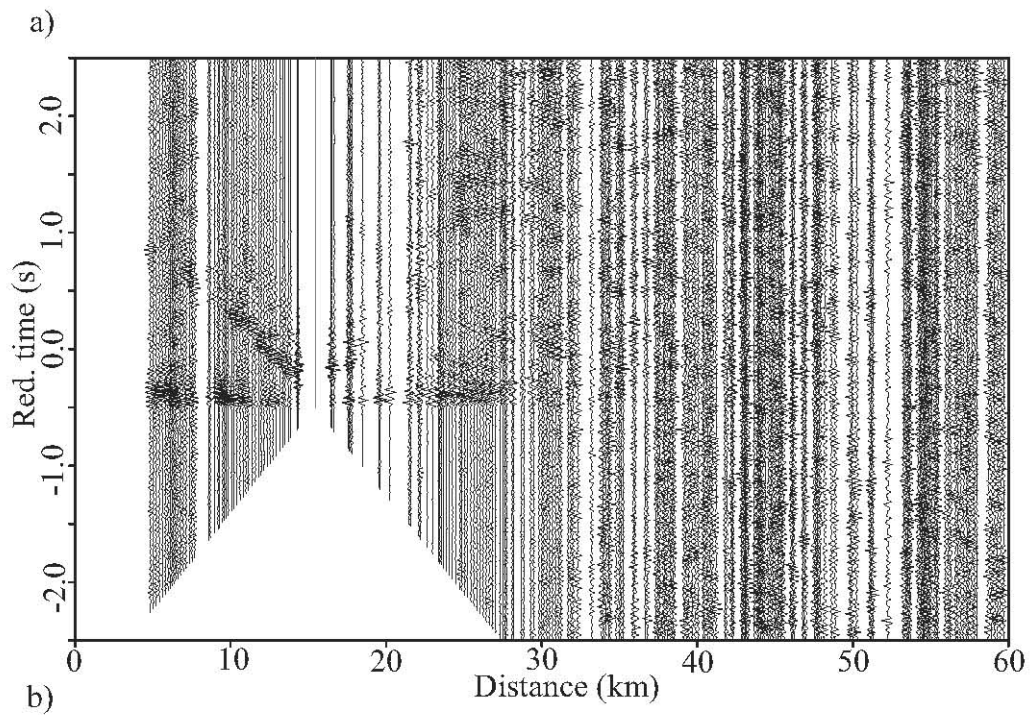
The recorded data was stacked from 100 m intervals to 1 km intervals to improve signal-to-noise ratio. The stacked data was correlated with the sweep signal and processed into common receiver gathers for each recording station. The sweep signal used for correlation was recorded with one portable station.

The processed data were compiled into record sections for all the recording stations (Fig. 2). Afterwards we analyzed the seismograms visually and picked arrival times of major refracted and reflected phases manually. Whenever possible, we tried to use non-filtered traces for picking. However, in some cases we had to filter the data by 20–36 Hz band-pass filter, in order to improve the signal-to-noise ratio of the secondary phases.

The first arrivals of P-waves ( $P_g$ ) can be observed at offsets up to 20–60 km in the record sections. In addition, several secondary arrivals of the reflected P-waves can be recognized (Figs. 2 and 3). The first intra-crustal reflection ( $PC_1$ ) is seen on almost every record section. The second intra-crustal reflection ( $PC_2$ ) can be seen in record sections of most stations, except from stations 1 and 10–13. The third intra-crustal reflection ( $PC_3$ ) is clearly visible in record sections of stations 2, 4 and 7. In addition, a number of arrivals from deeper interfaces in the crust can be recognized (Figs. 2 and 3). Reliable phase correlation was not possible, because these arrivals were only seen at few traces. The data quality is the best in the central part and the worst in the northern end of the profile, where the sites are noisy. Our estimate of the uncertainty of the picked traveltimes is about 0.05 s. The quality of S-waves was generally poor. The clearest S-wave arrivals can be seen at station 2 (Fig. 2a). The travel times of the first arrival P-waves are also plotted in a offset-reduced traveltime plot in Fig. 4.

#### 4. *P-wave velocity models*

The traveltimes of reflected and refracted waves were used to obtain a P-wave velocity model of the uppermost crust along FIRE4 profile. In our study, we used trial-and-error fit of measured and calculated travel times using forward raytracing by SEIS83 package (Červený and Pšenčík, 1983), with graphical interfaces by Zelt (1994) and Komminaho (1998), and also the traveltime inversion using Rayinvr code by Zelt and Smith (1992). The starting model for both methods was a three-layer 1-D velocity model, with layer boundaries at depths of 1 km and 3 km, and with vertical velocity gradient within each layer.



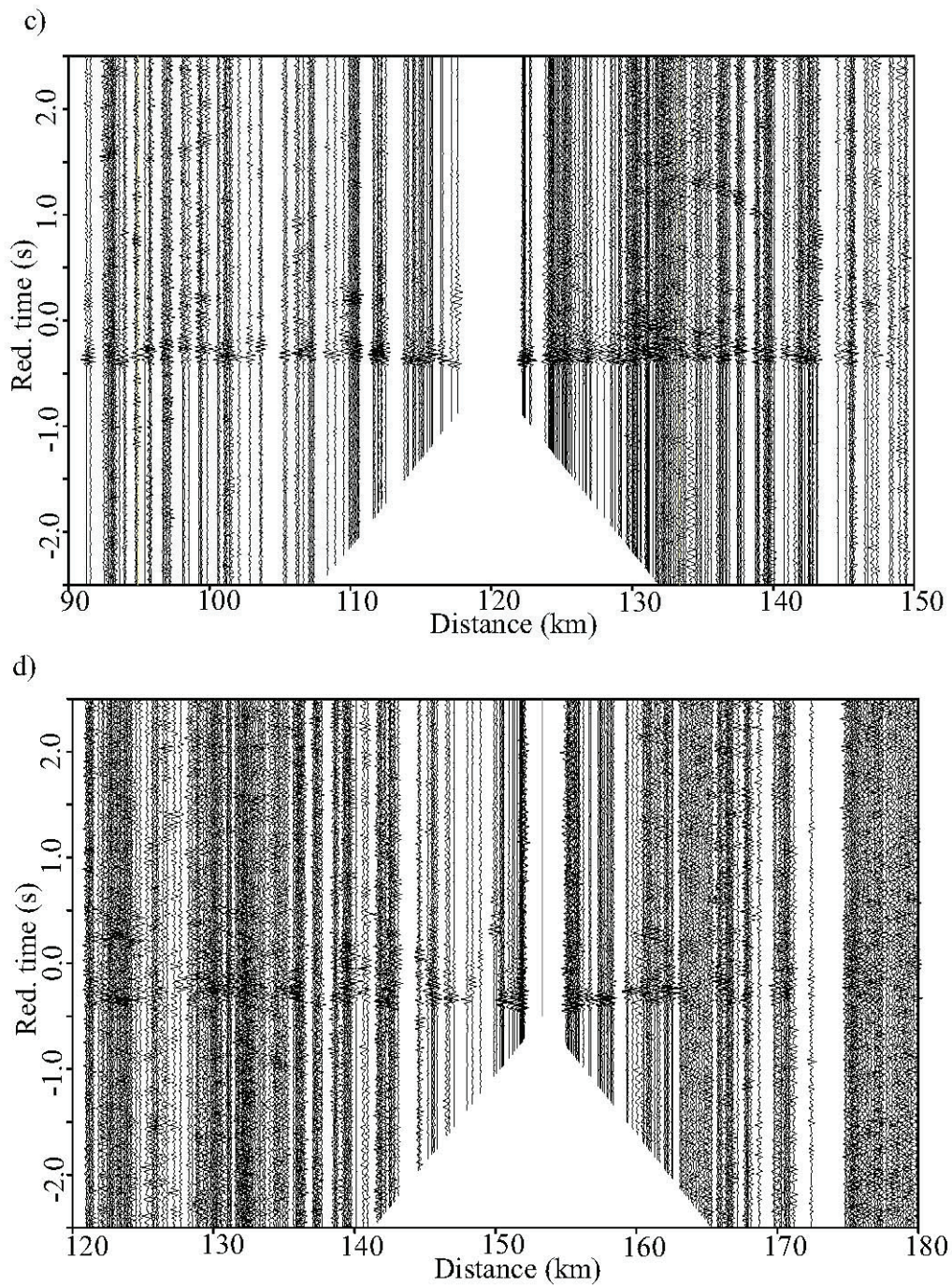
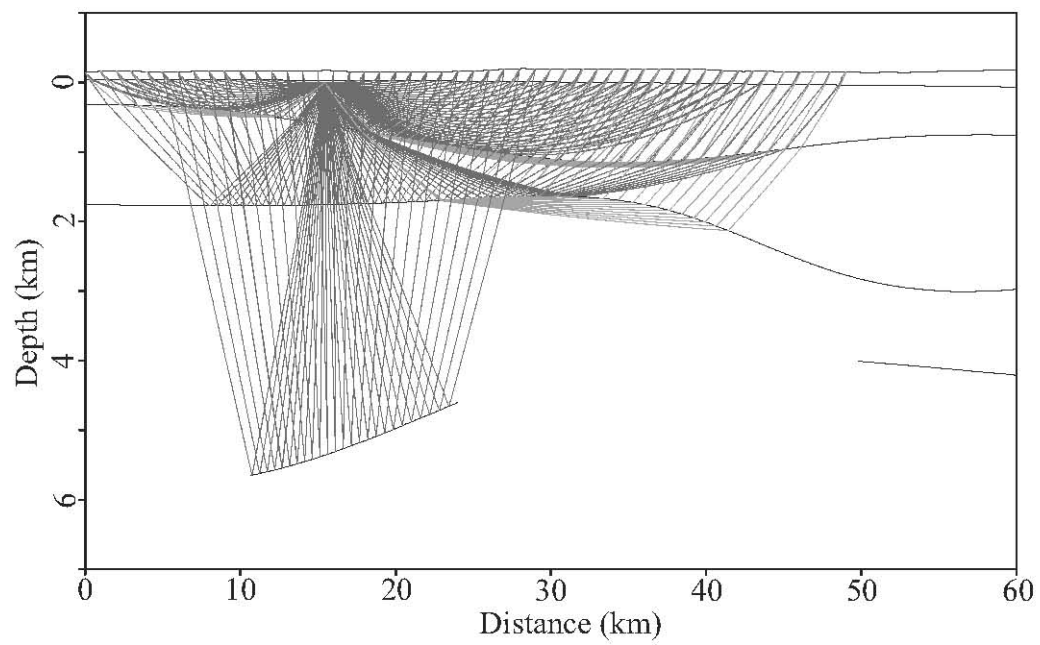
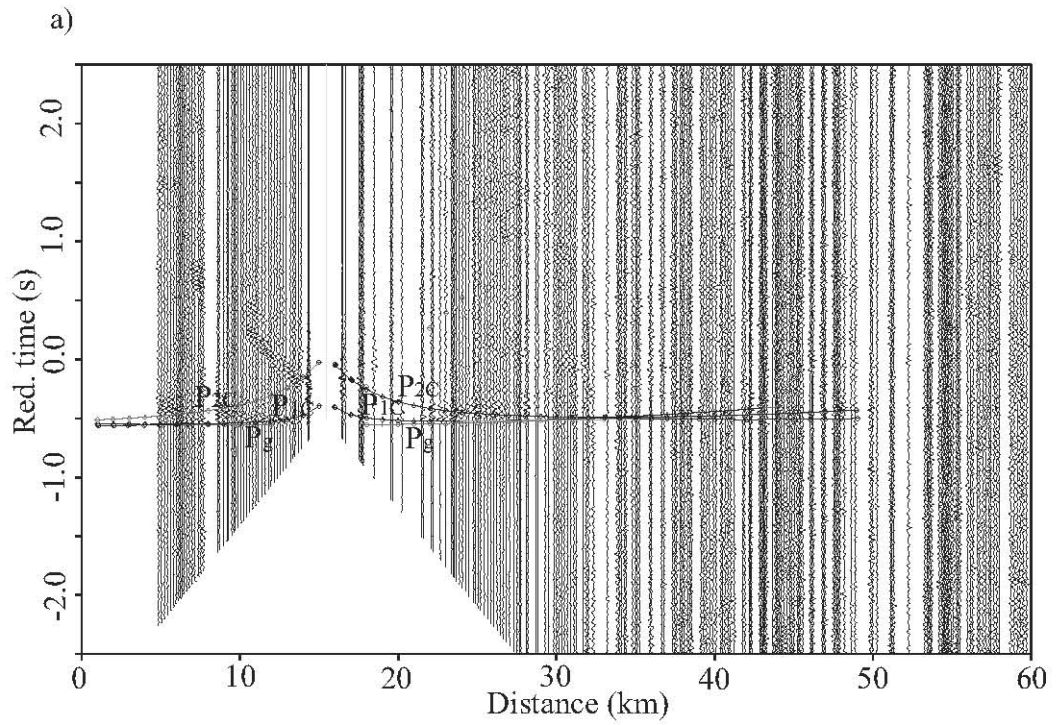


Fig. 2. Wide-angle record sections of the FIRE4 Vibroseis experiment. The reduction velocity is 6.0 km/s. No frequency filter is used, but only every second trace has been plotted for imaging purposes. Common receiver gathers are shown for stations a) 2, b) 5, c) 7, and d) 9 (see Fig. 1. for the location of the stations).



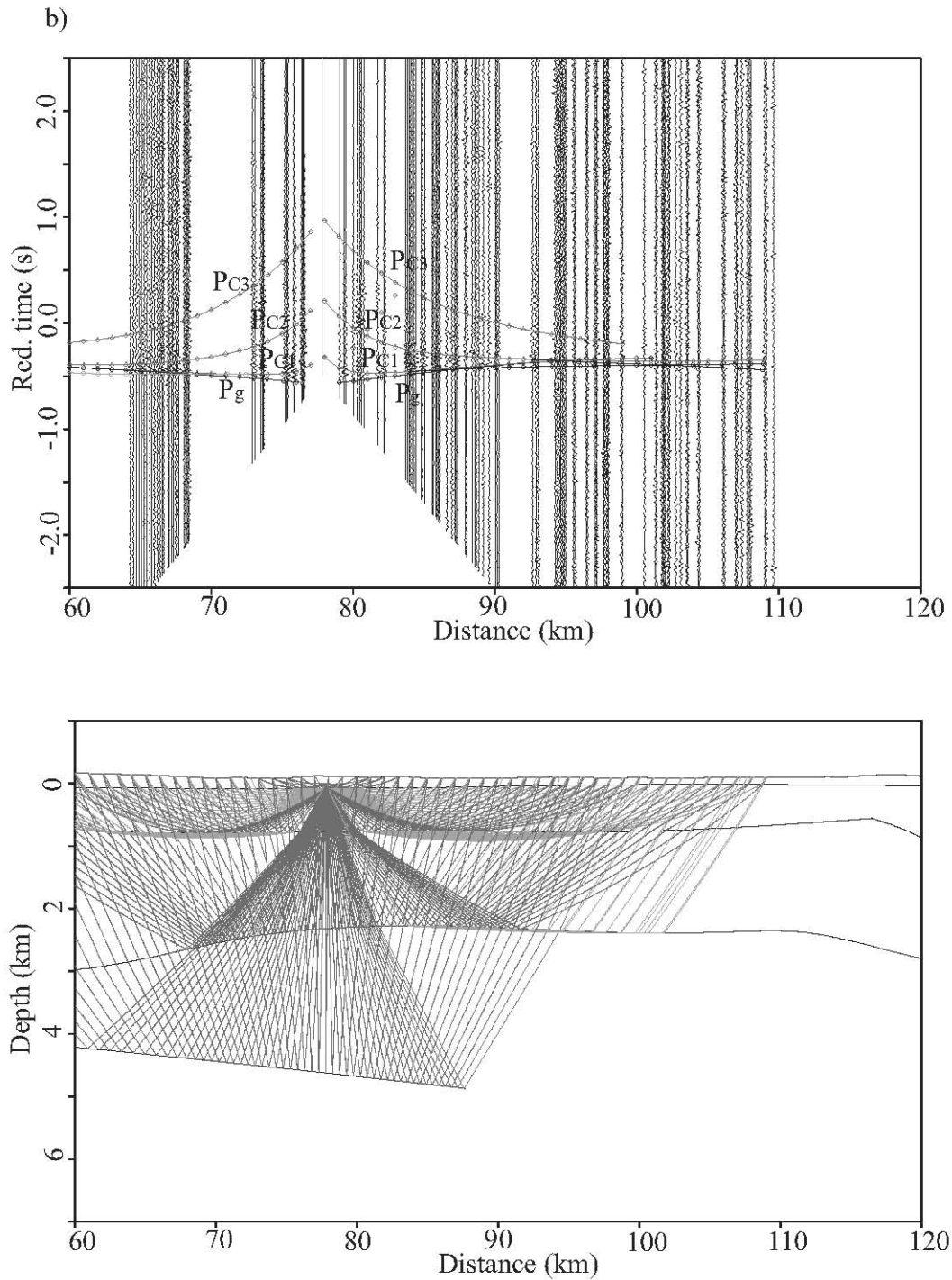


Fig. 3. The ray tracing results of four receiver points. Each subplot contains two panels. The upper panel contains a record section with calculated traveltimes plotted with lines. The first arrivals and two or three reflections from the crust (depending on receiver point) are marked with  $P_g$ ,  $P_{1C}$ ,  $P_{2C}$ , and  $P_{3C}$ , respectively. The lower panel shows ray-paths for the final raytracing model with vertical exaggeration ratio 1:5. The subplot (a) corresponds to the receiver point 2, (b) to 5, (c) to 7, and (d) to 9 (see Fig. 1 for receiver point locations).



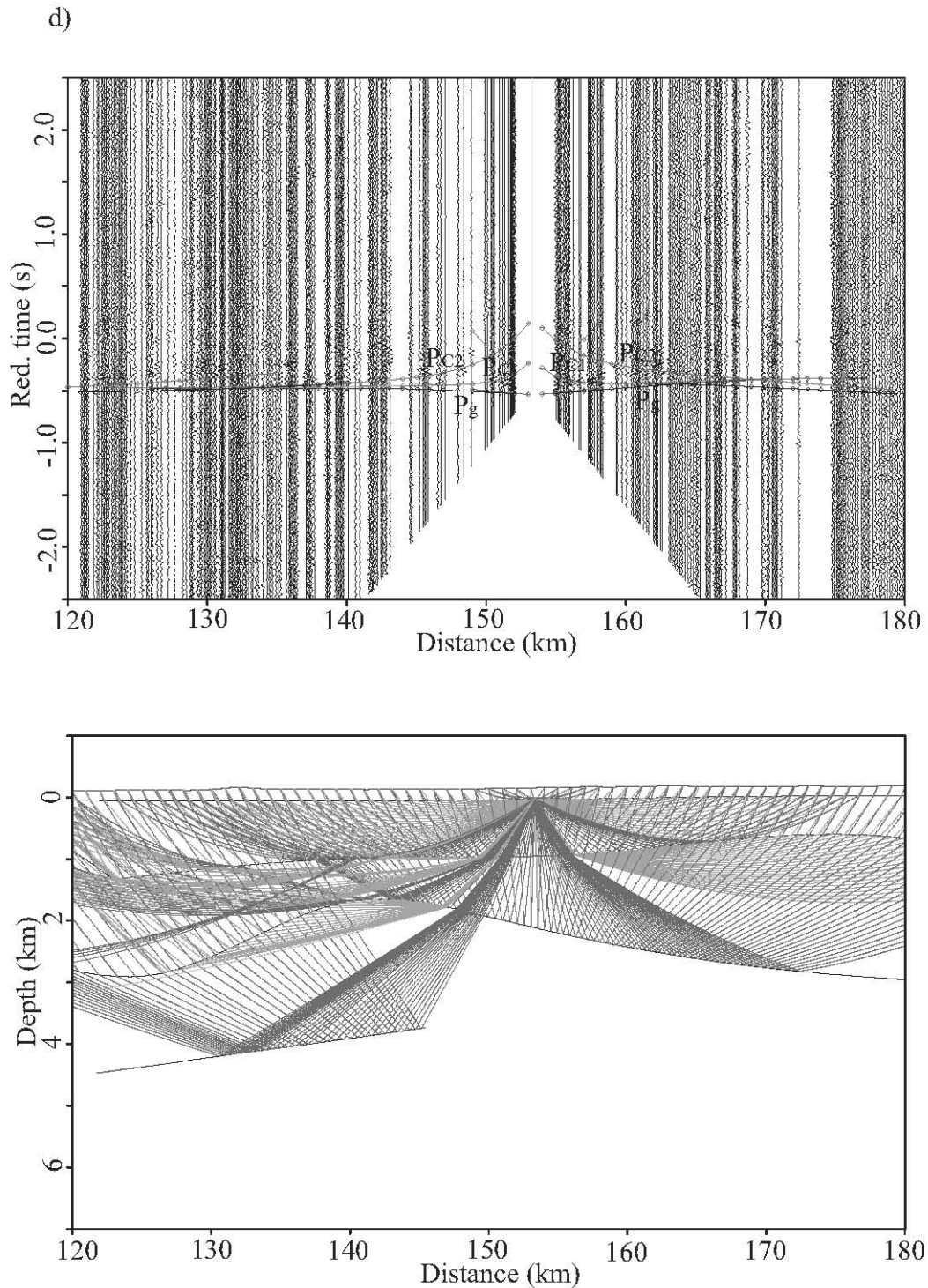


Fig. 3. The ray tracing results of four receiver points. Each subplot contains two panels. The upper panel contains a record section with calculated traveltimes plotted with lines. The first arrivals and two or three reflections from the crust (depending on receiver point) are marked with  $P_g$ ,  $P_{1C}$ ,  $P_{2C}$ , and  $P_{3C}$ , respectively. The lower panel shows ray-paths for the final raytracing model with vertical exaggeration ratio 1:5. The subplot (a) corresponds to the receiver point 2, (b) to 5, (c) to 7, and (d) to 9 (see Fig. 1 for receiver point locations).

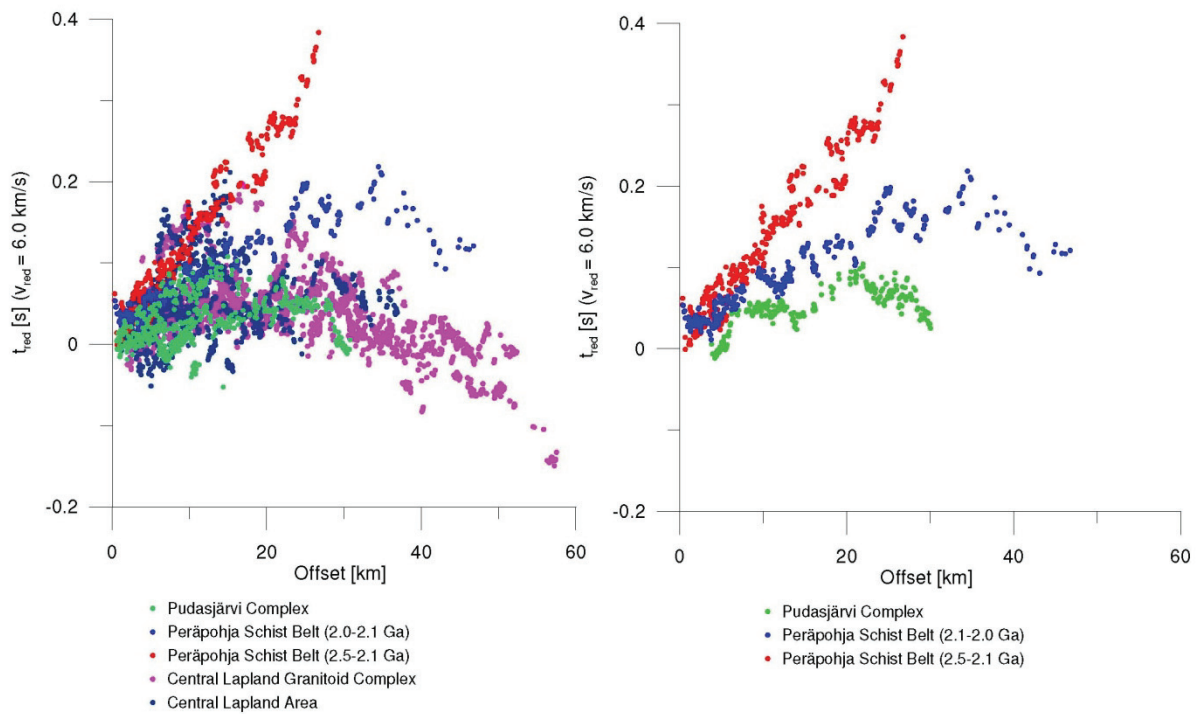


Fig. 4. The first arrival traveltimes – offset comparison for all receiver points. Reduction velocity is 6.0 km/s. All the measured first arrivals are shown in the left panel. Different colours are used for rays travelling in the different geological units. The right panel contains only receiver points on Peräpohja Schist Belt.

#### 4.1 Forward raytrace modelling with SEIS83

A starting model was created and modified with a model program (Komminaho, 1998) and synthetic traveltimes were calculated with the SEIS83 raytracing program (Červený and Pšenčík, 1983; Komminaho, 1998). Synthetic traveltimes were compared to wide-angle reflection and refraction recordings of FIRE4 profile with the ZPLOT program (Zelt, 1994, Fig. 3). The measured traveltimes were corrected for the topography effect, although the maximum difference in elevation along the profile was only 150 m.

Final trial-and-error P-wave velocity model of FIRE4 profile extends to the depth of 5 km (Fig. 5) and has three sub-horizontal boundaries. The depth to the first boundary is close to 1 km, while the depth to the second boundary varies between 1.8 km and 2.5 km. The third boundary is defined from reflectors at depths between 4 km and 5 km, but these reflectors could only be traced at few recording stations. The traveltimes calculated from final model fit well to the data (Fig. 3).

The lateral velocity variations correlate well with the main geological units observed at the surface. In the second layer the P-wave velocity is 5.90 km/s between recording stations 1 and 3 (the Pudasjärvi Complex), while it is 5.70 km/s between the stations 3 and 5 (the Peräpohja Schist Belt). The P-wave velocity is 5.85 km/s between the stations 5 and 10 (the Central Lapland Granitoid Complex), and it is 5.75 km/s between the stations 10 and 13. The velocities in the deeper layer follow similar pattern,

although the effect of the Peräpohja Schist Belt seems to be restricted to upper 2 km (Fig. 5a). One of the most pronounced features in a model is the area of high velocities (up to 6.3 km/s) inside the Central Lapland Granitoid Complex, limited from the top by a boundary at the depth of 2 km.

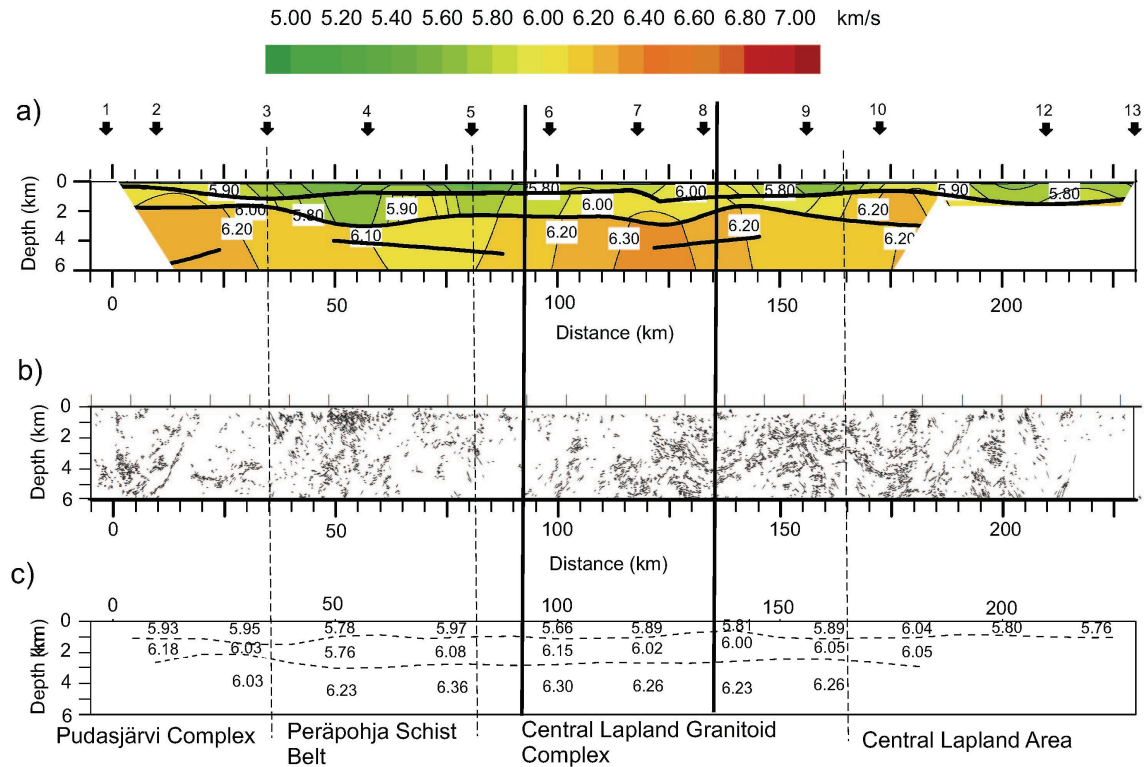


Fig. 5. P-wave velocity models with vertical exaggeration ratio 1:3.3. (a) A ray tracing model of FIRE4. The receiver points are marked with arrows. (b) An automatic line drawing of FIRE4 reflection profile after *Pattison et al.*, 2006. (c) A Rayinvr model of FIRE4. The main geological units are marked below the figures and their boundaries are marked with dashed line throughout all models. The area of the gravity models (Fig. 8 (g), (h), and (i)) is shown with black lines.

#### 4.2 *Traveltimes inversion using Rayinvr*

In the inversion of P-wave traveltime data we used the Rayinvr code by *Zelt and Smith* (1992). With Rayinvr both the model boundaries and the seismic velocity structure can be optimized simultaneously. The program uses a shooting method to find the ray paths through the velocity model. The damped least-squares inversion is used to determine the updated model parameters.

The inversion grid was composed of 10 km wide cells. The height of the cell was the distance between the upper and lower layer boundary. The P-wave velocities in the nodes of these cells and coordinates of the nodes in the (x,z) coordinate system (where z is depth and x is the distance along the profile) were taken as model parameters and the velocity inside the cells was linearly interpolated.

The software calculates standard errors of the uncertainties of the model parameters. These calculated errors should be considered as the lower boundary of the

true parameter errors. They are due to the uncertainties of the traveltimes picks and they do not take into account the correlations between the model parameters, phase identification errors, or errors due to approximation of real 3D velocity distribution by a 2D model (Zelt and Smith, 1992).

The initial model was defined as described in Section 4.1. The reflectors at the depths between 4 and 5 km were not included in the inversion, because there were not data from all receivers. The uncertainties of the traveltimes were assumed to be equal to the picking uncertainty (0.05 s) and uncertainties of the velocities and depths of the boundary nodes were assumed to be 0.10 km/s and 0.10 km, respectively. The value of 1.0 was used for overall damping factor. In the inversion, the vertical gradients inside the layers were set to be constant, while the P-wave velocities and layer thicknesses were optimized. Layer boundary smoothing was used.

In order to reduce the amount of free parameters in the inversion procedure, the inversion was performed separately for each layer, starting from the top layer. The final result of the inversion is shown in Figure 6. The position of the boundaries, as well as the velocities in the upper layers, are generally in a good agreement with the results of the forward raytrace modelling (Fig. 5a,c).

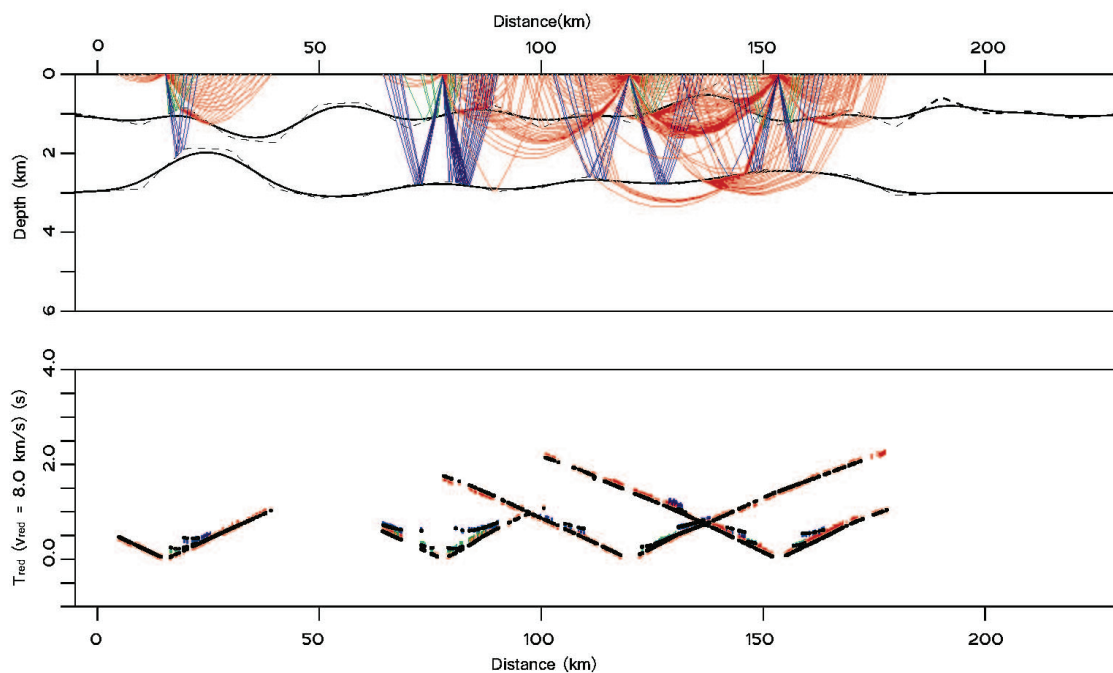


Fig. 6. A Rayinvr P-wave velocity inversion model. The upper panel shows the final inversion model with vertical exaggeration ratio 1:10. The black lines show the boundaries with smoothing and dashed lines without smoothing. The rays traced for receiver points 2, 5, 7, and 9 are plotted. The lower panel shows the measured traveltimes (red, green, and yellow dots) and calculated traveltimes (black dots). The reduction velocity is 8.0 km/s.

The RMS traveltimes residual of final model is 0.036 s and the corresponding normalized  $\chi$ -squared value is 0.533. The calculated model uncertainty is presented in Fig. 7. The uncertainty of the P-wave velocities varies almost only in vertical direction and grows from 0.04 km/s near surface to 0.12 km/s at the bottom of the model (depth

of 6 km). The uncertainty in the deeper part of the model could even be larger in reality, as there are almost no direct rays and no reflected rays deeper than 3.5 km. In contrast, the uncertainty of the boundary depths varies mainly in lateral direction between 0.03 km and 0.10 km. The largest uncertainty corresponds to the areas of large changes of velocity in vertical direction (Fig. 7).

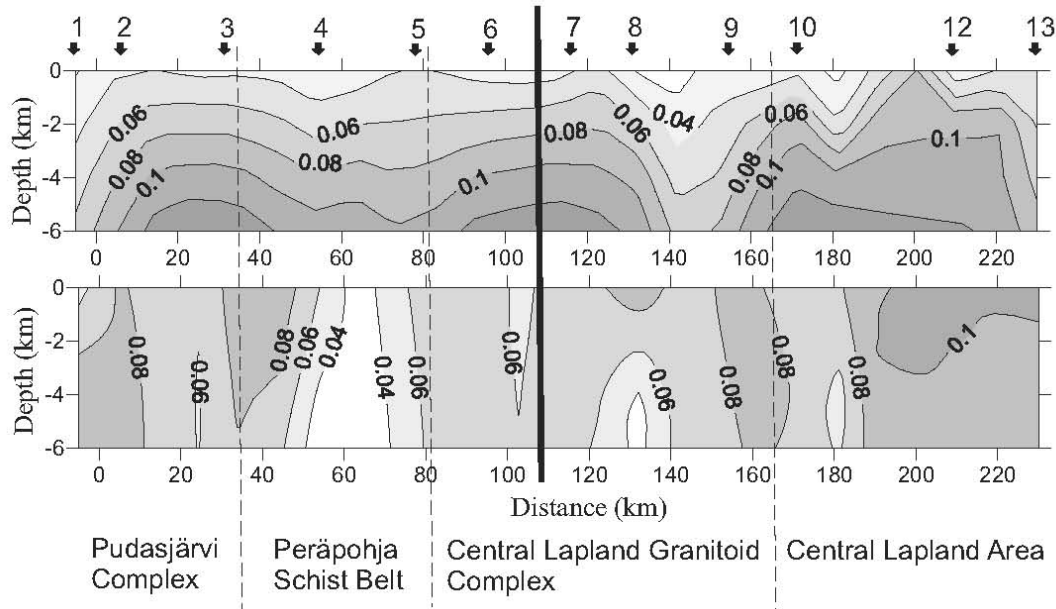


Fig. 7. The calculated errors of Rayinvr P-wave velocity inversion. The upper panel shows the standard error of the P-wave velocity (km/s) and the lower panel shows the standard error of the boundary depth (km). The vertical exaggeration ratio in both panels is 1:6.6.

## 5. 3D gravity inversion

For the gravity inversion, the most interesting problem was the velocity maximum at the distance of about 115 km in Fig. 5a. The area of high velocities is limited by the top boundary at the depth of about 2 km. In the geological map, there are no boundaries between receiver points 7 and 8 (Fig. 1a), but there is a pronounced maximum of Bouguer anomaly there (Fig. 1c). This anomaly has been interpreted earlier, but without use of seismic information. As the gravity modelling is generally ambiguous, the previous studies provided diverse estimates of the depth to the source of this anomaly (e.g. Hahn and Bosum, 1986, Korhonen et al., 2002). In our study, we used seismic velocity model and petrophysical information in order to constrain gravity modelling.

### 5.1 Bouguer anomaly map and density data

In our study, we used the digital Bouguer anomaly map compiled by the Geological Survey of Finland from the results of gravity measurements collected by the Finnish Geodetic Institute (Fig. 1b, Korhonen et al., 2002). The average linear spacing between the observation stations was 5 km. The Bouguer anomaly map used in our study was obtained using interpolation of this data into a 8 km x 8 km regular grid (Elo,

1997; Kääriäinen and Mäkinen, 1997; Korhonen *et al.*, 2002). The coordinate system is the National Finnish Coordinate System (KKJ) (Hirvonen, 1949; Ollikainen *et al.*, 2001).

The digital map of the surface bulk density (Fig. 1c) was compiled from results of laboratory measurement of density of rock samples collected all over Finland (Korhonen *et al.*, 1997). As the sampling points were not evenly distributed (particularly in our study area), the density map was obtained by interpolation of the raw data to a regularly spaced grid of 8 km x 8 km. The density values in the nodes of the grid were obtained as weighted sum of density at points closest to the node. We also excluded all sampling points taken from dykes. The dykes are small in volume, but they formed the majority of samples in some parts of the research area. This can affect significantly the average density obtained by interpolation. In particular, the mafic dykes of the Peräpohja Schist Belt and the Central Lapland Area produced quite large artificial density anomalies within these areas; therefore, we excluded these samples from further consideration.

## 5.2 Gravity inversion technique and software

For the 3D gravity inversion we used the interactive computer program Grablox by Pirttijärvi *et al.* (2004). The Grablox uses two major inversion methods, namely, singular value decomposition (SVD) and Occam inversion (Hjelt, 1992). In each method there are three possible ways to parameterise the model (height, density and height + density inversions). In the density inversion, the sizes of the blocks are kept constant and the densities of the blocks are optimised. In the height inversion, the densities and the horizontal sizes of the blocks are fixed and block heights are optimised. For the density outside the study area we have used the mean-layer background density method, in which the density surrounding the research area is defined separately as the mean density of each elementary layer inside a model.

The starting model was made by selecting about 100 km x 300 km x 8 km block as the area for density modelling (Fig. 1). The research area was approximated by 8 km x 8 km x 0.5 km blocks of constant density. The initial model had the density of 2670 kg/m<sup>3</sup> in all blocks, except the surface layer where the density values were adopted from the petrophysical data base of the Geological Survey of Finland (Fig. 1c).

The regional gravity field was calculated from an existing density model by Kozlovskaya *et al.* (2004) (Fig 8a). As our study area is situated inside the region sampled by this model, the effect of large geological units outside the area could be taken into account in this way. The even larger scale regional effects from the deep crust and mantle were modelled with so-called base anomaly  $g_b$  defined by equation:

$$g_b = g_0 + (x - x_0)dg_x + (y - y_0)dg_y \quad (1)$$

where  $g_0$  is the base anomaly at the south western corner of the research area with coordinates  $x_0$  (east-west direction) and  $y_0$  (north-south direction) and  $dg_x$  and  $dg_y$  the gradients of the base anomaly. These values for our research area were found using

Grablox. They are  $g_0 = -12.89$  mgal,  $dg_x = 3.36$  mgal/100 km and  $dg_y = 8.23$  mgal/100 km (Fig. 8b).

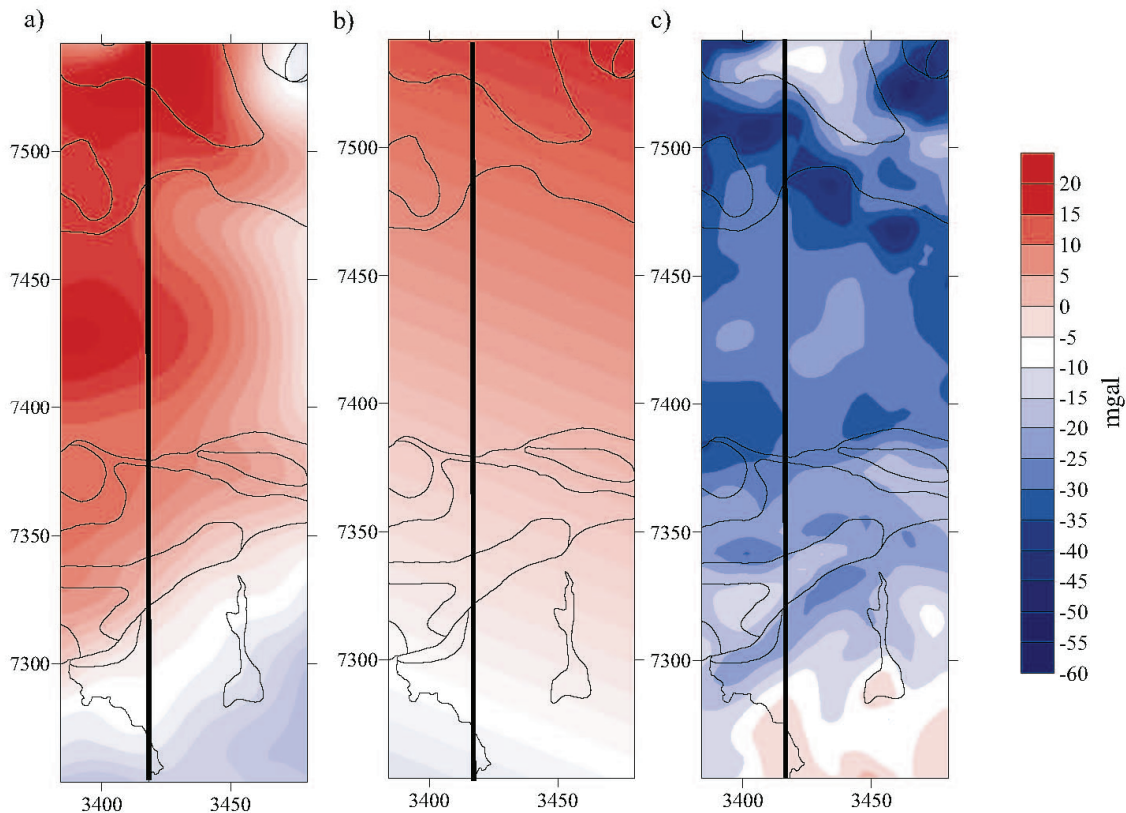


Fig. 8. The regional and residual Bouguer anomaly maps. The subplot (a) shows the regional anomaly calculated from previous large scale model by *Kozlovskaya et al.*, 2004, the subplot (b) shows the base anomaly calculated with Grablox software, and the subplot (c) shows the residual anomaly after regional anomaly is excluded from Bouguer anomaly.

### 5.3 Gravity inversion and modelling

In the inversion of the gravity data we used the residual of the Bouguer anomaly after subtraction of the regional field and the base anomaly. The Occam inversion method was used (*Hjelt*, 1992). As described earlier, the densities in the surface layer were interpolated from the petrophysical data. Because the surface samples might not represent the densities within this thick layer (0.5 km) correctly, we calculated the height inversion in the surface layer before the density inversion. After this, the density inversion was done in the other layers, while the densities in the surface layer were fixed. The final model of this study is shown in Fig. 9a,d, and e. The RMS error of this model is 0.481 mgal and the maximum difference between the observed and calculated Bouguer data is 16 mgal. These maximum differences can only be seen near the Kittilä Greenstone Belt in the northern part of a model, where changes in Bouguer anomaly are sharp. The Occam inversion always implies some smoothing and thus cannot account for such strong contrasts. In the other parts of the model, the difference is generally less than 4 mgal.

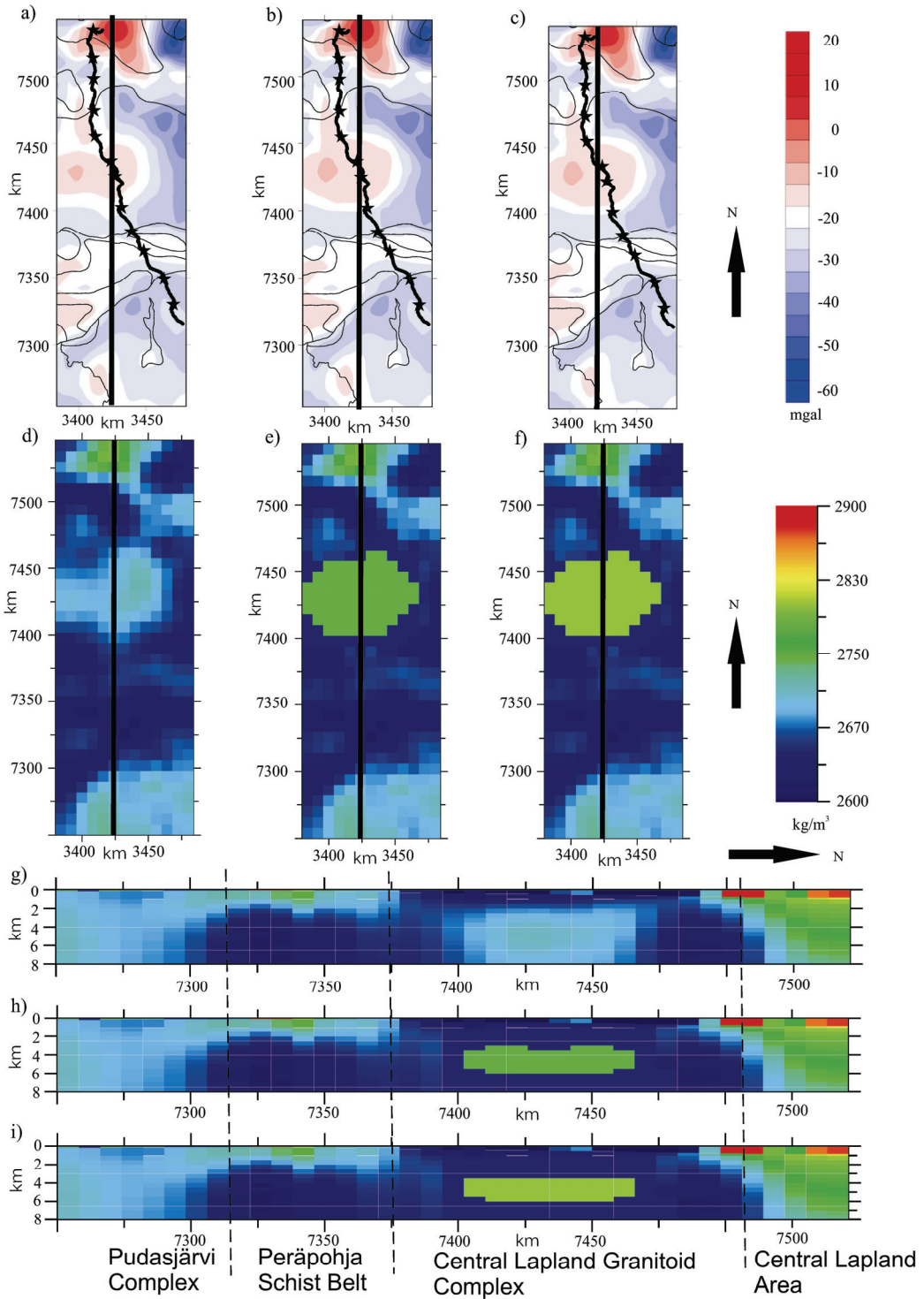


Fig. 9. A result of gravity inversion and forward modelling. A calculated Bouguer anomaly model of the research area for a) Occam inversion, b) trial-and-error modelling with body density  $2780 \text{ kg/m}^3$ , and c) trial-and-error modelling with body density  $2800 \text{ kg/m}^3$ , respectively. In the subplots, the borders of geological units and location of FIRE4 and recording points are shown. The subplots (d), (e), and (f) contain the horizontal sections of a models at the depth of 5 km in the same order as with Bouguer anomaly maps. The subplots (g), (h), and (i) contain the vertical sections of a model from south (left) to north (right) close to FIRE4 profile in the same order as Bouguer anomaly maps. The exaggeration ratio is 1:3.3. The location of the vertical sections is also shown on Bouguer anomaly maps (a-c) and horizontal density model sections (d-f) as black line. The boundaries of the main geological units are indicated with dashed lines in vertical sections (g-i).

All the main geological units from the geological map can be seen also in the density model. There are two high density bodies that extend to the surface. The first one is the Peräpohja Schist Belt that is about 2 km thick. The thickness of the second one, the Kittilä Greenstone Belt, is mostly 4 km but reaches almost 8 km in its deepest point. In addition, there are two high density bodies that do not extend to the surface on our model: the first one is located within the Pudasjärvi Complex, where a thin layered mafic intrusion (*Weihed et al., 2005*) is marked on the geological map (Fig. 1). The body could indicate the magma source of the intrusion but it is too near the border of our model to model with higher precision. The other one, located in the middle of the Central Lapland Granitoid Complex, was the main target for the gravity inversion.

It is very likely, that the body inside the Granitoid Complex has sharper density contrast with surrounding than the Occam inversion can model, because it has delimited by the boundary with strong velocity contrast in P-wave velocity model (Fig. 5a). In addition, FIRE4 reflection seismic section shows some strong reflectors at the depth of 3 km at the distance of 125 km (Fig. 5b). This may indicate presence of a sharp lithological boundary with a high density contrast. In order to test this hypothesis, we used the forward gravity modelling. The P-wave velocity of about 6.30 km/s (Fig. 5a) often implies densities of 2780–2800 kg/m<sup>3</sup> (*Christensen and Mooney, 1995*).

Moreover, *Kern et al. (1993)* reported such values for Proterozoic intrusive diorites and also for one sample of sheared metasedimentary granulite from northern Finland. This density range was used to verify the values of density and depth for the body obtained in the earlier Occam inversion with trial-and-error method. Initially the densities inside the Lapland Granitoid Complex were changed to the average value of 2650 kg/m<sup>3</sup>. This value was acquired from a model obtained by Occam inversion. Then a body with constant density was added to this averaged model. For this body we used two different values of density (2780 and 2800 kg/m<sup>3</sup>, respectively).

Both final models (Fig. 9) have the RMS errors that are only slightly larger than that for Occam model. Some errors on the edges of the high density body were anticipated because the modelling was done with relatively large 8 km x 8 km block size in horizontal direction. The maximum difference between the observed Bouguer data and the calculated data in the Granitoid Complex is only about 5 mgal, compared to about 3 mgal in Occam inversion model. The RMS value for the models with densities of 2780 kg/m<sup>3</sup> and 2800 kg/m<sup>3</sup> is 0.517 mgal and 0.513 mgal, respectively.

## 6. Results

Though the conditions were not favourable during the data acquisition, the first arrivals and reflections from boundaries in the uppermost crust in FIRE4 wide-angle reflection and refraction data could be traced to the offsets of 20–60 km. The data quality was the best in the middle of the profile.

The maximum depth extent of the P-wave velocity models is about 5 km with both reflected and refracted waves and 3 km with only refracted waves. Velocity models obtained independently by forward raytracing and by inversion (Fig. 5a and 5c,

respectively) demonstrate similar features of the velocity distribution within the upper crust and differ only in details. The boundaries detected by FIRE4 wide-angle data are partly coincident with the reflection events seen in FIRE4 near-vertical reflection sections (Fig. 5b). Good coincidence is observed especially for the central part of the profile (the Central Lapland Granitoid Complex), where the quality of the wide-angle data is good. The main geological units can easily be recognized (in particular, in the trial-and-error model, Fig. 5a). There are significant differences in P-wave velocities between recording stations. When measured traveltimes are all plotted on the same offset-reduced traveltimes plot, one can distinguish even quite small velocity differences between crustal units (Fig. 4). In particular, the two age groups of the Peräpohja Schist Belt can be easily recognized, as the older part of the Belt has significantly lower velocities than the younger part.

The main geological units can be distinguished also in a density model together with some smaller features (Fig. 9a,d and e). There is also a high density inside Central Lapland Granitoid Complex corresponding with a P-wave velocity maximum in our P-wave velocity model (Fig. 5a). The 3D gravity inversion and modelling showed that the source of this anomaly is at the depth of 3 km and that it continues to the depth of about 6 km. It stretches approximately between distances 7400 km and 7450 km in the north-south direction and between distances 3400 km and 3450 km in the east-west direction (Fig. 9a, d). As the Occam inversion includes always some smoothing, the boundaries of the body became quite blurred. Thus it is likely that the density obtained is biased towards smaller values. In spite of that, the density in the middle of the body is about  $2720 \text{ kg/m}^3$ , whereas it is about  $2650 \text{ kg/m}^3$  in the other parts of the Central Lapland Granitoid Complex. Therefore, the density model obtained by the Occam inversion and velocity models are in a good agreement.

The more precise position of the anomalous body in the middle of the Central Lapland Granitoid Complex was obtained by trial-and error modelling. The upper boundary of the body with the density of  $2780 \text{ kg/m}^3$  is at 3 km (Fig. 9b, e, h) and the upper boundary of the body with the density of  $2800 \text{ kg/m}^3$  is at 3.5 km (Fig. 9c, f, i). The lower boundary of the body is located at 6 km in both models. As we pointed out earlier, these values may correspond either to granodiorite or metasedimentary granulite. However, high reflectivity of this body seen in the reflection section of FIRE4 profile implies that it is composed of strongly deformed and folded rocks with contrasting elastic properties.

## 7. Discussion and conclusions

Reflection seismic Vibroseis technique is a very effective tool for studying the detailed structure of the crust. It should be remembered, however, that this method provides information only on one property of rock, namely, reflectivity. As was shown by *Hurich et al.* (2001) and *Berzin et al.* (2002), there are many reasons for reflectivity in the crust, ranging from lithological contacts to change in metamorphic grade. Moreover, structural boundaries of geological units do not always coincide with the

reflections seen in the reflection sections. Thus geological interpretations based on only one rock property (reflectivity) may be non-unique (*Benn et al.*, 2006). The only geological interpretation of the southern part of FIRE4 profile (*Patison et al.*, 2006) was based on the reflection section, geological maps, and regional scale geophysical maps, without modelling of potential fields. That is why it did not explain origin of many details of reflectivity in the upper crust, including the high-reflectivity area beneath the Central Lapland Granitoid Complex. Our study shows that this reflectivity corresponds to true lithological contact between high velocity, high density rocks overlaid by low density granitoid rocks observed at the surface. The boundary between them is seen clearly in a model obtained from wide-angle data and also in a density model. Thus taking into consideration information on velocity and density can improve significantly the quality of geological interpretation of reflection data.

Comparison of wide-angle and near vertical reflection recordings of Vibroseis sources was made recently by *Fomin and Goleby* (2006). They concluded that these two data types map different features of the media. Our study does not support this conclusion. The wide-angle data from Vibroseis sources used in our study contain reflection events with the same dominating frequency (2–36 Hz) as near-vertical recordings. Our model shows good spatial agreement between areas of high reflectivity in wide-angle data and reflection seismic sections.

Our study showed that recordings of Vibroseis sources registered by 1 Hz and 2 Hz geophones can be effectively used for the purpose of velocity modelling in the uppermost crust. Horizontal stacking of recordings of several Vibroseis sources improves significantly signal to noise ratios. That enables the recognition of not only the first arrivals, but also the secondary arrivals of reflected and refracted waves. In our study, the modelling of reflected and refracted waves generated by Vibroseis sources made it possible to recover P-wave velocity inhomogeneities in the upper crust down to a depth of 5 km. The quality and the resolutions of wide-angle Vibroseis data is sufficient to distinguish between different lithological units in the upper crust based on velocity differences. Therefore, the method complements efficiently traditional reflection seismic surveys and can be used to investigate the detailed structure in the uppermost crust.

### *Acknowledgements*

The authors would like to thank Riitta Hurskainen and staff of the SGO for help with the software. The digital gravity map used was compiled by J. Korhonen from the gravity data by Finnish Geodetic Institute and Geological Survey of Finland. The authors thank Dr. M. Pirttijärvi for the softwares Bloxer and Grablox. Hanna Silvennoinen would like to thank the Geological Survey of Finland for possibility to use the digital geological map of the Fennoscandian Shield in her PhD work. Hanna Silvennoinen would also like to thank Tauno Tönningin säätiö for funding the part of the research. The authors would also like to thank the reviewers Annakaisa Korja and Ilmo Kukkonen for their valuable suggestions and comments.

*References*

- Benn, K., J.-C. Mareschal and K. Condie, K. (Eds.), 2006. *Archean geodynamics and environments*. Geophysical monograph **164**. American Geophysical Union. United States of America. 320 pp.
- Berzin, R.G., Yu.G. Yurov and N.I. Pavlenkova, 2002. CDP and DSS data along the Uchta-Kem profile (the Baltic Shield). *Tectonophysics*, **355**, 187–200.
- Blundel, D.J., 1990. Seismic images of continental lithosphere. *J. Geol. Soc.*, **147**, 895–913.
- Bois, C., M. Cazes, A. Hirn, A. Mascle, P. Matte, L. Montadert and B. Pinet, 1988. Contribution of deep crustal profiling to the knowledge of the lower crust in France and neighbouring areas. *Tectonophysics*, **145**, 253–275.
- Brown, L., M. Barazangi, S. Kaufmann and J. Oliver, 1986. *The first decade of COCORP: 1974-1984: AGU Geodynamics Series*, **13**, 107–120.
- Červený, V. and Pšenčík, I., 1983. SEIS83 – numerical modelling of seismic wave fields in 2-D laterally varying structure by the ray method. In: Engdahl, E.R. (Ed.), Documentation of Earthquake algorithms, World Data Cent., *A Solid Earth Geophys.*, pp. 36–40. Rep. **SE-35**.
- Christensen, N.I. and W.D. Mooney, 1995. Seismic velocity structure and composition of the continental crust: A global view. *Journal of Geophysical Research*, vol. **100**. No. B7, 9761–9788.
- Daly, J.S., V.V. Balagansky, M.J. Timmerman and M.J. Whitehouse, 2006. The Lapland-Kola orogen: Palaeoproterozoic collision and accretion of the northern Fennoscandian lithosphere, in *European Lithosphere Dynamics*, edited by D.G. Gee and R.A. Stephenson, Geological Society, London, Memoirs 32, pp. 579–598.
- DEKORP-Research Group, 1985. First results and preliminary interpretation of deep reflection seismic recordings along profile DEKORP 2-South. *J. Geophys.*, **57**, 137–163.
- DEKORP-Research Group, represented by Flueh E.R., Klaeschen D. and Meissner R., 1990. Wide-angle Vibroseis Data from the Western Rhenish Massif. *Tectonophysics*, **173**, 83–93.
- Eilu, P., P. Sorjonen-Ward, P. Nurmi and T. Niiranen, 2003. A Review of Gold Mineralization Styles in Finland. *Economic Geology*, **98**, 1329–1353.
- Elo, S., 1997. Interpretation of the gravity map of Finland. *Geophysica* **33**(1), 51–80.
- Fomin, T. and B.R. Goleby, 2006. Lessons from a joint interpretation of vibroseis wide-angle and near-vertical reflection data in the north-eastern Yilgarn, Western Australia. *Tectonophysics*, **420**, 301–316.
- Gaál, G. and R. Gorbatshev, 1987. An outline of the Precambrian evolution of the Baltic Shield. *Precambrian Research*, **35**, 15–52.
- Gaál, G., A. Berthelsen, R. Gorbatshev, R. Kesola, M. Lehtonen, M. Marker and P. Raase, 1989. Structure and composition of the Precambrian crust along the POLAR profile in the northern Baltic Shield. *Tectonophysics*, **162**, 1–25.

- GTK, 2003. GTK/Suomenkallioperä 1:10 000 000. [HTML-file.] [Read 15.10.2007.] <http://www.gtk.fi/palvelut/info/kartat/kp10-milj.htm>
- Hahn, A. and W. Bosum, 1986. Geomagnetism: selected examples and case histories. *Geoexploration Monographs*, Series 1, no. 10, 166 p.
- Hirvonen, R.A., 1949. Die Gauss-Krügerische Projektion für breite Meridian streifen auf dem Internationalen Ellipsoide. *Suomen Geodeettisen laitoksen julkaisuja*, **36**, Helsinki, Finland.
- Hjelt, S.-E., 1992. *Pragmatic inversion of geophysical data*. Springer –Verlag. Germany. 262 pp.
- Huhma, H., T. Mutanen and M. Whitehouse, 2004. Oldest rocks of the Fennoscandian Shield: the 3.5 Ga Siurua trondhjemite gneiss in the Archaean Pudasjärvi Granulite Belt, Finland. In Abstracts of the 14th Annual V. M. Goldschmidt Conference, Copenhagen, Denmark, June 5–11, 2004. *Geochimica et Cosmochimica Acta*, **68**, A754.
- Hurich, C.A., S.J. Deemer, A. Indares and M. Salisbury, 2001. Compositional and metamorphic controls on velocity and reflectivity in the continental crust: An example from the Grenville Province of eastern Quebec. *Journal of Geophysical Research* **106**(B1): doi: 10.1029/2000JB900244.
- Janik, T., E. Kozlovskaya, P. Heikkinen, J. Yliniemi and H. Silvennoinen, 2009. Evidence for preservation of crustal root beneath the Proterozoic Lapland-Kola orogen (northern Fennoscandian shield) derived from P- and S-wave velocity models of POLAR and HUKKA wide-angle reflection and refraction profiles and FIRE4 reflection transect. *J. Geophys. Res.* **114** B06308, doi:10.1029/2008JB005689.
- Kern, H., C. Walther E.R. Flüh and M. Marker, 1993. Seismic properties of rocks exposed in the POLAR profile region – constraints on the interpretation of the refraction data. *Precambrian Research*, **64**, 169–187.
- Koistinen, T., M.B. Stephens, V. Bogatchev, Ø. Nordgulen, M. Wennerström and J. Korhonen, 2001. Geological map of Fennoscandian shield, scale 1:2 000 000. Geological Surveys of Finland, Norway and Sweden and the North-West Department of Natural Resources of Russia.
- Komminaho, K., 1998. Software manual for programs MODEL and XRAYS – a graphical interface for SEIS83 program package. *University of Oulu, Division of Geophysics*, Report No. **20**, 31 pp.
- Korhonen, J., H. Säävuori and L. Kivekäs, 1997. Petrophysics in the crustal model program of Finland. In: Autio, S. (Ed.), 1997. Geological Survey of Finland, Current Research 1995–1996, *GSF, Special Paper* **23**, 157–173.
- Korhonen, J.V., S. Aaro, T. All, S. Elo, L.Å. Haller, J. Kääriäinen, A. Kulinich, J.R. Skilbrei, D. Solheim, H. Säävuori, R. Vaher, L. Zhdanova and T. Koistinen, 2002. Bouguer Anomaly Map of the Fennoscandian Shield 1 : 2 000 000. Geological Surveys of Finland, Norway, and Sweden and Ministry of Natural Resources of Russian Federation.

- Kozlovskaya, E., S. Elo, S.-E. Hjelt, J. Yliniemi, M. Pirttijärvi and SVEKALAPKO STWG, 2004. 3D density model of the crust of southern and central Finland obtained from joint interpretation of SVEKALAPKO crustal P-wave velocity model and gravity data. *Geoph. J. Int.*, **158**, 827–848.
- Kukkonen, I.T., Heikkinen, P., Ekdahl, E., Hjelt, S.-E., Ylineimi, J., Jalkanen, E. and FIRE Working Group, 2006. Acquisition and geophysical characteristics of reflection seismic data on FIRE transects, Fennoscandian Shield. In: Kukkonen, I.T. and R. Lahtinen (Eds.), 2006. Finnish Reflection Experiment FIRE 2001–2005. *Geological Survey of Finland*, Special paper **43**. pp. 13–43.
- Kääriäinen, J. and J. Mäkinen, 1997. The 1979–1996 gravity survey and results of the gravity survey of Finland. *Publications of the Finnish Geodetic Institute*, **125**, 24 p.
- Lahtinen, R., A.A. Garde and V.A. Melezhik, 2008. Paleoproterozoic evolution of Fennoscandia and Greenland, *Episodes*, **31**, 1, 1–9.
- Lehtinen, M., P. Nurmi and O. Rämö (Eds.), 2005. Precambrian geology of Finland: key to the evolution of the Fennoscandian shield. Elsevier.
- Luosto, U., S.M. Zverev, I. Kosminskaya and H. Korhonen, 1980. Observations of Fennolora shots on additional lines in Finnish Lapland. General Assembly of European Seismological Commission, Budapest, Proceedings and Activity Report.
- Luosto, U., E. Lanne, H. Korhonen, A. Guterch, M. Grad, R. Materzok and E. Perchuc, 1984. Deep structure of the Earth's crust on the SVEKA profile in central Finland, *Annales Geophysicae*, **2**, 559–570.
- Ollikainen, M., H. Koivula and M. Poutanen, 2001. EUREF-FIN -koordinaatisto ja EUREF-pistetihennykset Suomessa. *Finnish Geodetic Inst.*, Tiedote **24** (in Finnish).
- Patison N.L., A. Korja, R. Lahtinen, V.J. Ojala and FIRE Working Group, 2006. FIRE seismic reflection profiles 4, 4A and 4B: Insights into the crustal structure of northern Finland from Ranua to Näätämö. In: Kukkonen, I.T. and R. Lahtinen, 2006. Finnish Reflection Experiment FIRE 2001–2005. *Geological Survey of Finland*, Special paper **43**.
- Pirttijärvi M., E. Kozlovskaya, S. Elo, S.-E. Hjelt and J. Yliniemi, 2004. 3-D geophysical crustal model of Finland. In: Ehlers, C., O. Eklund, A. Korja, A. Kruuna, R. Lahtinen and L. Pesonen, 2004. Listosphere 2004. Programme and extended abstracts. pp. 101–103.
- Rühl, T. and E. Lühschen, 1990. Inversion of first-break traveltime data of deep seismic reflection profiles. *Geophysical Prospecting*, **38**, 247–266.
- Walther, Ch. and E.R. Flüh, 1993. The POLAR Profile revisited: combined P-and S-wave interpretation. *Precambrian Research*, **64**, 153-168.
- Weihed, P., N. Arndt, K. Billström, J.-C. Duchesne, P. Eilu, O. Martinsson, H. Papunen and R. Lahtinen, 2005. 8: Precambrian geodynamics and ore formation: The Fennoscandian Shield. *Ore Geology Reviews*, **27**, 273–322.

Zelt, C.A. and R.B. Smith, 1992. Seismic traveltimes inversion for 2-D crustal velocity structure, *Geophysical Journal International*, 108, 16–34.

Zelt, C.A., 1994. ZPLOT – An interactive plotting and picking program for seismic data. Bullard lab, Univ. of Cambridge, UK.